Chapter 1

CMS-EXO-16-012: a CMS mono-Higgs analysis (3.2 fb^{-1})

S. Ahn, J. Park and W. Zhang

Abstract
We present the implementation and validation of the CMS-EXO-16-012 analysis within MADANALYSIS 5. This search targets events featuring a large missing transverse momentum and the signature of a Higgs boson decaying into a pair of bottom quarks or photons, and focuses on 2.3 fb^{-1} of proton-proton collisions at a center-of-mass energy of 13 TeV. In our reimplementation, we only focus on the $\gamma\gamma$ final state and validate our reimplementation in the context of a two-Higgs-doublet model including an extra neutral gauge boson.

1 Introduction

In this document, we detail the MADANALYSIS 5 [1–3] implementation of the CMS search for the associated production of dark matter with a Higgs boson decaying into a $b\bar{b}$ or $\gamma\gamma$ pair. This search focuses on the analysis of 2.3 fb^{-1} of proton-proton collision data at a center-of-mass energy of $\sqrt{s}$ = 13 TeV [4]. The $b\bar{b}$ channel subanalysis is divided in two regimes, *i.e.* a resolved regime where the Higgs boson decays into two distinct reconstructed b-jets, and a Lorentz-boosted regime where the Higgs boson is reconstructed as a single fat jet. In this last case, the signal extraction is performed through a simultaneous fit of signal regions and background-enriched control regions. We have not been able to reproduce this fit consequently to the lack of associated public information, and we have therefore not reimplemented this analysis strategy. On the other hand, the $\gamma\gamma$ channel search is performed by seeking an excess of events over the Standard Model expectation in the diphoton mass spectrum, which solely relies on a cut-and-count approach.

The analysis presented in Ref. [4] has been interpreted using a benchmark simplified model in which a two-Higgs-doublet model is supplemented by an extra Z' boson and a dark matter particle χ (Z'-2HDM) [5, 6]. The signal that is probed by the analysis corresponds to the resonant production of a heavy Z' vector boson which further decays into a Standard-Model-like Higgs boson h and an intermediate heavy pseudoscalar boson A that connects the visible sector to a dark sector. The mediator A hence decays into a pair of dark matter particles. The entire process,

$$pp \to Z' \to hA \to h\,\bar{\chi}\chi\ , \tag{1.1}$$

is described in Fig. 1.1. However, this signature is quite generic and its reimplementation within the MADANALYSIS 5 framework could enable more reinterpretations. For example it could be used to probe other scalar extensions of the Standard Model, noteworthy in a more general two-Higgs-doublet plus singlet extensions of the Standard Model or in a supersymmetric context. In particular, such as signature could provide an interesting handle on the NMSSM, where the $Z'Ah$ coupling is replaced by a A_1A_2h or $h_3h_2h_1$ interaction with $A_{1,2}$ and $h_{1,2,3}$ respectively being CP-odd and CP-even scalars [7].

2 Description of the analysis

To enforce the compatibility with the presence of a Higgs boson decaying into two photons, events are selected if they feature a photon pair satisfying given invariant mass and transverse momentum (p_T) requirements. Moreover, fake photons are rejected through constraints on the calorimetric activity of the

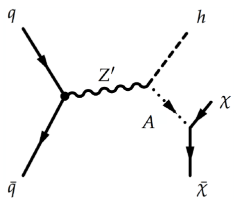

Fig. 1.1: Leading order Feynman diagram yielding the production of the signal of interest in the considered Z'–2HDM simplified model. The associated signature consists of a Higgs boson produced in association with missing transverse momentum.

reconstructed photons and their isolation. The signal region is further defined by imposing constraints on the ratio of the photon p_T to the diphoton invariant-mass, as well as on the missing transverse momentum and on the angular separation between the reconstructed Higgs boson and the missing momentum.

2.1 Objects definition and preselection

In this analysis, photons are identified following different ways. A cut-based identification is first performed, relying on a loose working point. The exact selections are presented in Ref. [8], as well as in the CMS-PAS-EXO-16-012 analysis note [4]. In practice, isolation is imposed by restricting the calorimetric activity in a cone of radius $\Delta R = 0.3$ centered on the photon through three variables, $I_\pm$, I_0 and I_γ. These respectively correspond to the amount of calorimetric deposits originating from charged hadrons, neutral hadrons and photons lying in the considered cone.

The signal region is defined by requiring the presence of two photons whose transverse momenta fulfill

$$p_T(\gamma_1) > 30 \text{ GeV} \qquad \text{and} \qquad p_T(\gamma_2) > 18 \text{ GeV}. \tag{1.2}$$

Fake photons are rejected by requiring that the ratio of the amount of energy deposited in the hadronic calorimeter is of at most 10% of the amount of energy deposited on the electromagnetic calorimeter,

$$H/E < 0.1 \ , \tag{1.3}$$

and photon isolation is ensured by the selections on the $I_\pm$, I_0 and I_γ variables given in Table 1.1. Whilst the isolation requirement related to the neutral particles should include the so-called ρ correction that accounts for the dependence of the pileup transverse energy density on the photon pseudorapidity, ρ being the median of the transverse energy density per unit area, we ignore this correction in our implementation due to the lack of relevant information.

Events are finally further preselected by requiring that the invariant mass of the diphoton system satisfies

$$m_{\gamma\gamma} > 95 \text{ GeV} \ , \tag{1.4}$$

in order to be compatible with the decay of a Higgs boson.

2.2 Signal selections

After the preselection described above, the CMS-PAS-EXO-16-012 analysis includes a series of cuts defining the signal region. These kinematic selections consist of additional constraints on the p_T of the two photons,

$$\frac{p_T(\gamma_1)}{m_{\gamma\gamma}} > 0.5 \qquad \text{and} \qquad \frac{p_T(\gamma_2)}{m_{\gamma\gamma}} > 0.25 \ , \tag{1.5}$$

for the leading and next-to-leading photon respectively, and of a selection on the diphoton transverse momentum and on the missing transverse energy E_T^{miss},

$$p_{T_{\gamma\gamma}} > 90 \text{ GeV} \qquad \text{and} \qquad E_T^{\text{miss}} > 105 \text{ GeV}. \tag{1.6}$$

Variable	Barrel	Endcap
$I_\pm$ [GeV]	< 3.32	< 1.97
I_0 [GeV]	$< 1.92 + 0.14 p_T^\gamma + 0.000019 (p_T^\gamma)^2$	$< 11.86 + 0.0139 p_T^\gamma + 0.000025 (p_T^\gamma)^2$
I_γ [GeV]	$< 0.81 + 0.0053 p_T^\gamma$	$< 0.83 + 0.0034 p_T^\gamma$

Table 1.1: Requirements imposed on the photon isolation. We distinguish photons reconstructed in the barrel (second column) and in the endcap (third column), and p_T^γ denotes the photon transverse momentum.

Two extra cuts further constrain the angular seperation between the missing transverse momentum $\mathbf{p}_T^{\rm miss}$ and the diphoton system,

$$|\Delta\phi(\gamma\gamma,\,\mathbf{p}_T^{\rm miss})| > 2.1 \qquad \text{and} \qquad \min_j(|\Delta\phi(j,\,\mathbf{p}_T^{\rm miss})|) > 0.5\ , \tag{1.7}$$

where the minimization has to account for all jets with a transverse momentum larger than 50 GeV. In this analysis, jets are recontructed by means of the anti-k_T algorithm [9], with a radius parameter set to $R = 0.4$. Finally the diphoton invariant mass is further imposed to satisfy

$$120\ \text{GeV} < m_{\gamma\gamma} < 130\ \text{GeV}\ . \tag{1.8}$$

3 Validation

In order to validate our reimplementation, we focus on the Z'–2HDM model described above and on the production of a heavy Z' boson that decays into a Higgs boson and a pair of dark matter particles via an intermediate pseudoscalar state A (see Fig. 1.1 for a representative Feynman diagram). Hard-scattering signal events are generated with MADGRAPH5_aMC@NLO [10], the matrix elements being generated from the model information provided through an appropriate UFO [11] model shared by CMS and convoluted with the next-to-leading-order set of NNPDF 3.0 parton densities [12]. Our tests focus on several benchmark scenarios featuring each a different Z'-boson mass $M_{Z'}$. The simulation of the hadronic environment (parton showering and hadronization) is performed by means of PYTHIA 8 [13], that is also used to handle the decay of the final-state Higgs boson. The simulation of the response of the CMS detector is achieved via DELPHES 3 [14], that internally relies in FASTJET [15] for object reconstruction, with an tuned detector configuration including updated b-tagging and reconstruction performances.

We make use of our reimplementation of the CMS-PAS-EXO-16-012 analysis to compute MADANALYSIS 5 predictions for the acceptance times efficiency values for the different scenarios. Our reimplementation is then validated by comparing our results with the official numbers from CMS.

3.1 Event Generation

Hard scattering events are generated by making use of the MADGRAPH5_aMC@NLO package, together with the UFO model available on the CMS public repository,
http://rkhurana.web.cern.ch/rkhurana/monoH/models/
The necessary configuration files for each of the considered benchmarks can be found from the MADGRAPH5 generator repository of CMS,
https://github.com/cms-sw/genproductions/tree/mg240/bin/MadGraph5_aMCatNLO
in the folder
cards/production/13TeV/monoHiggs/Zp2HDM/Zprime_A0h_A0chichi

We fix the masses of the pseudoscalar state and of the dark matter particle to 300 GeV and 100 GeV, respectively, and set the decay width of the pseudoscalar to 8.95 GeV. We investigate several configurations for the properties of the Z' boson. Its mass is hence varied and fixed to 600, 800,

$M_{Z'}$ (GeV)	600	800	1000	1200	1400	1700	2000	2500
$\Gamma_{Z'}$ (GeV)	11.223	15.765	20.225	24.624	28.982	35.473	41.927	52.639

Table 1.2: Values of the Z' total width for each benchmark point used in the validation process.

	Acceptance $\times$ efficiency $(A \cdot \epsilon)$		
$m_{Z'}$ (GeV)	CMS EXO-16-012	MA5	Difference
600	0.317 $\pm$ 0.004	0.355 $\pm$ 0.001	-11 %
800	0.399 $\pm$ 0.004	0.451 $\pm$ 0.001	-13 %
1000	0.444 $\pm$ 0.004	0.494 $\pm$ 0.001	-8.2 %
1200	0.474 $\pm$ 0.004	0.513 $\pm$ 0.001	-0.6 %
1400	0.492 $\pm$ 0.004	0.515 $\pm$ 0.001	-4.7 %
1700	0.493 $\pm$ 0.004	0.494 $\pm$ 0.001	-0.2 %
2000	0.351 $\pm$ 0.004	0.355 $\pm$ 0.001	-1.1 %
2500	0.213 $\pm$ 0.004	0.208 $\pm$ 0.001	2.3 %

Table 1.3: Comparison of the signal acceptance times efficiencies predictions made by MADANALYSIS 5 with the CMS official numbers. The difference is calculated according to Eq. (1.9).

1000, 1200, 1400, 1700, 2000 and 2500 GeV for the different setups. All the Z' couplings to Standard Model particles $g_{\rm SM}$ are chosen to be equal to 0.8, while the coupling to dark matter is fixed to 1 [6]. The corresponding Z'-boson width for each mass value is given in Table 1.2.

We enforce the Higgs boson to decay into a diphoton system by setting appropriately the PYTHIA 8 configuration. This requires to modify two PYTHIA 8 input files, `Pythia8CUEP8M1Settings_cfi.py` and `Pythia8CommonSettings_cfi.py`, which we have been again found on public repositories of the CMS generator group,
https://github.com/cms-sw/cmssw/tree/CMSSW_7_1_9_patch
https://github.com/cms-sw/cmssw/tree/CMSSW_7_2_X
respectively, in the `Configuration/Generator/python` subfolder in both cases.

Concerning the simulation of the CMS detector, we have slightly modified the configuration that has been designed for the reimplementation of the CMS-EXO-16-037 analysis and that is available on
http://madanalysis.irmp.ucl.ac.be/wiki/PublicAnalysisDatabase
Compared with the default settings, the b-tagging and lepton and photon reconstruction performances have been updated according to Refs. [8, 16]. In particular, we make use of the cMVAv2 loose b-tagging working point, which corresponding to a correct b-tagging efficiency of about 83% for a misidentification probability of about 10%. We have also defined the dark matter particle as an invisible state that does not deposit energy in the calorimeters.

3.2 Comparision with official results

As CMS has not provided detailed validation information, we have validated our implementation on the basis of the available material. We present the product of signal acceptance and selection efficiency for

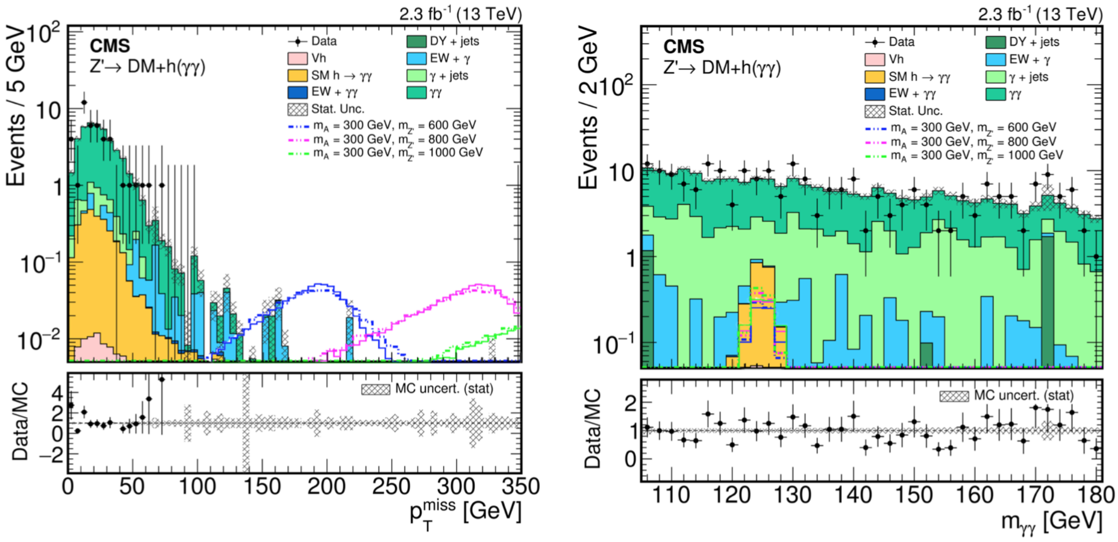

Fig. 1.2: Missing transverse energy (left) and diphoton invariant mass (right) distributions after all selection criteria have been imposed, except the one on the missing enegy (both cases) and the one of the diphoton invariant mass (right panel only). The dotted lines are the official CMS results taken from Ref. [4] and the solid lines are the MADANALYSIS 5 predictions.

each considered Z' mass point, and we define the difference with the official numbers as

$$\delta = 1 - \frac{(A \cdot \epsilon)^{\text{MA5}}}{(A \cdot \epsilon)^{\text{CMS}}} , \tag{1.9}$$

The results are given in Table 1.3.

Moreover, we present, for representative signal scenarios, the missing transverse energy and diphoton invariant mass distributions in Fig. 1.2 after normalizing our signal distributions similarly to CMS. For all performed tests, a good agreement is obtained.

4 Summary

In this note, we reported the MADANALYSIS 5 reimplementation of the CMS-EXO-16-012 and analysis and its validation. We compared signal selection efficicies times acceptance for varied benchmark scenarios, as well as two differential distributions. An overal agreement has been found, the differences being of at most 13%. This analysis is thus considered as validated and has been made available from MADANALYSIS 5 version 1.6 onwards, its Public Analysis Database and from INSPIRE [17],

http://doi.org/10.7484/INSPIREHEP.DATA.JT56.DDC3.1.

References

[1] E. Conte, B. Fuks, and G. Serret, *MadAnalysis 5, A User-Friendly Framework for Collider Phenomenology*, *Comput. Phys. Commun.* **184** (2013) 222–256, [arXiv:1206.1599]. 5

[2] E. Conte, B. Dumont, B. Fuks, and C. Wymant, *Designing and recasting LHC analyses with MadAnalysis 5*, *Eur. Phys. J.* **C74** (2014), no. 10 3103, [arXiv:1405.3982]. 5

[3] B. Dumont, B. Fuks, S. Kraml, S. Bein, G. Chalons, E. Conte, S. Kulkarni, D. Sengupta, and C. Wymant, *Toward a public analysis database for LHC new physics searches using MADANALYSIS 5*, *Eur. Phys. J.* **C75** (2015), no. 2 56, [arXiv:1407.3278]. 5

[4] **CMS** Collaboration, A. M. Sirunyan et al., *Search for associated production of dark matter with a Higgs boson decaying to* $\mathrm{b\bar{b}}$ *or* $\gamma\gamma$ *at* $\sqrt{s} = 13$ *TeV*, *JHEP* **10** (2017) 180, [arXiv:1703.05236]. 5, 6, 9

[5] A. Berlin, T. Lin, and L.-T. Wang, *Mono-Higgs Detection of Dark Matter at the LHC*, *JHEP* **06** (2014) 078, [arXiv:1402.7074]. 5

[6] D. Abercrombie et al., *Dark Matter Benchmark Models for Early LHC Run-2 Searches: Report of the ATLAS/CMS Dark Matter Forum*, arXiv:1507.00966. 5, 8

[7] S. Baum, K. Freese, N. R. Shah, and B. Shakya, *NMSSM Higgs boson search strategies at the LHC and the mono-Higgs signature in particular*, *Phys. Rev.* **D95** (2017), no. 11 115036, [arXiv:1703.07800]. 5

[8] **CMS** Collaboration, V. Khachatryan et al., *Performance of Photon Reconstruction and Identification with the CMS Detector in Proton-Proton Collisions at sqrt(s) = 8 TeV*, *JINST* **10** (2015), no. 08 P08010, [arXiv:1502.02702]. 6, 8

[9] M. Cacciari, G. P. Salam, and G. Soyez, *The Anti-k(t) jet clustering algorithm*, *JHEP* **04** (2008) 063, [arXiv:0802.1189]. 7

[10] J. Alwall, R. Frederix, S. Frixione, V. Hirschi, F. Maltoni, O. Mattelaer, H. S. Shao, T. Stelzer, P. Torrielli, and M. Zaro, *The automated computation of tree-level and next-to-leading order differential cross sections, and their matching to parton shower simulations*, *JHEP* **07** (2014) 079, [arXiv:1405.0301]. 7

[11] C. Degrande, C. Duhr, B. Fuks, D. Grellscheid, O. Mattelaer, and T. Reiter, *UFO - The Universal FeynRules Output*, *Comput. Phys. Commun.* **183** (2012) 1201–1214, [arXiv:1108.2040]. 7

[12] **NNPDF** Collaboration, R. D. Ball et al., *Parton distributions for the LHC Run II*, *JHEP* **04** (2015) 040, [arXiv:1410.8849]. 7

[13] T. Sjöstrand, S. Ask, J. R. Christiansen, R. Corke, N. Desai, P. Ilten, S. Mrenna, S. Prestel, C. O. Rasmussen, and P. Z. Skands, *An Introduction to PYTHIA 8.2*, *Comput. Phys. Commun.* **191** (2015) 159–177, [arXiv:1410.3012]. 7

[14] **DELPHES 3** Collaboration, J. de Favereau, C. Delaere, P. Demin, A. Giammanco, V. Lemaître, A. Mertens, and M. Selvaggi, *DELPHES 3, A modular framework for fast simulation of a generic collider experiment*, *JHEP* **02** (2014) 057, [arXiv:1307.6346]. 7

[15] M. Cacciari, G. P. Salam, and G. Soyez, *FastJet User Manual*, *Eur. Phys. J.* **C72** (2012) 1896, [arXiv:1111.6097]. 7

[16] **CMS** Collaboration, *Identification of b quark jets at the CMS Experiment in the LHC Run 2*, CMS-PAS-BTV-15-001. 8

[17] S. Ahn, J. Park, and W. Zhang, *Madanalysis5 implementation of the CMS search for Dark matter with large missing transverse momentum and a Higgs boson decaying to a pair of photons documented in arXiv: 1703.05236*, 10.7484/INSPIREHEP.DATA.JT56.DDC3.1. 9